

Fermi National Accelerator Laboratory

FERMILAB-Conf-94/023-E

DØ

The DØ Upgrade

**S. Gruenendahl
For the DØ Collaboration**

*University of Rochester
Rochester, New York 14627*

*Fermi National Accelerator Laboratory
P.O. Box 500, Batavia, Illinois 60510*

January 1994

**Presented at the 9th Topical Workshop on Proton-Antiproton Collider Physics,
Tsukuba, Japan, October 18-22, 1993**

Disclaimer

This report was prepared as an account of work sponsored by an agency of the United States Government. Neither the United States Government nor any agency thereof, nor any of their employees, makes any warranty, express or implied, or assumes any legal liability or responsibility for the accuracy, completeness, or usefulness of any information, apparatus, product, or process disclosed, or represents that its use would not infringe privately owned rights. Reference herein to any specific commercial product, process, or service by trade name, trademark, manufacturer, or otherwise, does not necessarily constitute or imply its endorsement, recommendation, or favoring by the United States Government or any agency thereof. The views and opinions of authors expressed herein do not necessarily state or reflect those of the United States Government or any agency thereof.

The DØ Upgrade*

The DØ Collaboration

presented by S. Gr̄ulendahl
Department of Physics and Astronomy
University of Rochester
Rochester, NY 14627

In order to maximize the physics potential of the Fermilab Tevatron proton antiproton collider complex, both the accelerator system and the two large collider detectors are undergoing major upgrades during the remainder of this decade. For the DØ detector [1], the upgrade focuses on implementation of an integrated magnetic tracker in the central region of the detector, accompanied by those modifications to other parts of the apparatus necessary to cope with the increase in interaction rate provided by the collider.

Physics Goals

Substantial increases in integrated luminosity per running period are required to achieve substantial improvements in knowledge of high P_T phenomena. Examples of the DØ physics goals for the next round of collider runs during the second half of this decade are [2-6]:

- The measurement of M_W , with a significantly reduced error, of order $\mathcal{O}(50 \text{ MeV})$, competitive with or better than the measurement expected from LEP200.
- Study of production and decay properties of the top quark; as figure 1 shows, a top mass determination error of $\mathcal{O}(5 \text{ GeV})$ roughly matches a 50 MeV M_W error in leverage on the range of allowed Higgs masses.
- A precision determination of the weak mixing angle from the forward-backward asymmetry in leptonic Z^0 decays.

These measurements will allow consistency checks of the standard model within a single experiment. Such studies will be complementary to the direct searches for new phenomena, which will continue to be a major part of the DØ high P_T physics program. Other areas of continued interest, which would benefit from a substantial increase in the size of experimental data samples, are:

- Studies of the strong interaction in (associated) production of intermediate vector bosons

*Talk given at the 9th Topical Workshop on Proton-Antiproton Collider Physics, Tsukuba, Japan, October 18-22, 1993

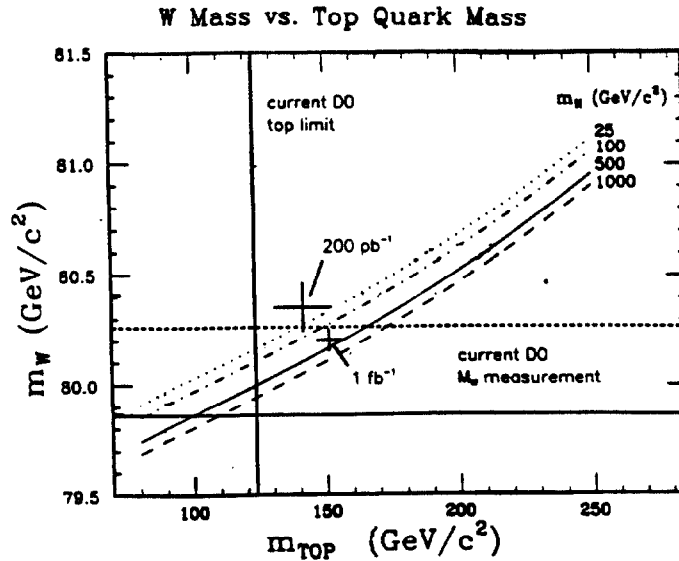


Figure 1: m_W, m_{Top} (plus $m_Z^{\text{LEP}}, \sin^2 \theta_W^{\text{Q}}$): measurement errors vs. m_{Higgs} dependence

Run period	$\int \mathcal{L} dt$ [pb^{-1}]	peak Lum. [$\text{cm}^{-2}\text{s}^{-1}$]	Δt_{bunch}	N_{bunch}
Ia 92/93	30	$7 \cdot 10^{30}$	$3.5 \mu\text{s}$	6 + 6
Ib 93/94	100	$1.9 \cdot 10^{31}$	$3.5 \mu\text{s}$	6 + 6
IIa 96/97	150	$2.2 \cdot 10^{31}$	400 ns	36 + 36
IIb 98/99	1000	10^{32}	400 ns or 132 ns	36 + 36 or 99 + 99

Table 1: Tevatron Parameters

- Investigation of the nucleon structure, in particular improvements in the knowledge of the gluon structure function, and quantitative differentiation between different parameterizations of quark structure functions.

This evolution of physics goals centered on high transverse momentum phenomena will be accompanied by the emergence of B physics studies at the hadron collider.

Tevatron Parameters

In order to achieve the necessary order of magnitude increase in luminosity which the DØ high P_T and B physics program requires, a multistep upgrade program of all components of the Tevatron accelerator complex is being pursued. For run Ib, currently starting, the linac has been upgraded. For the running period IIa, expected to start in the fall of 1996, an increase in the number of proton and antiproton bunches is planned. The last third of the decade will then see operation of the new main injector, which will make it possible to achieve data samples corresponding to several hundred events per picobarn during a running period. Table 1 lists the projected evolution of Tevatron parameters with time.

Elements of the DØ Detector Upgrade

Being a $\bar{p}p$ detector of the second generation, designed and built during a time when first experience was already gathered operating detectors in a hadron collider environment at the CERN Sp \bar{p} S and later also at the FNAL Tevatron, many features and design choices of the DØ apparatus are still to be regarded as optimized with respect to the physics goals and high luminosity operation. The uranium liquid argon calorimetry, full muon coverage, the modular multilayer trigger, and the readout system with independent parallel streams for different elements of the detector are examples. Nevertheless, adaptation to the shorter bunch crossing interval and the higher trigger and readout rates is necessary. Important parameters of the upgraded accelerator in this area are, besides the instantaneous luminosity, the 132 ns bunch crossing separation and the 2.1 μ s interaction-free gap in the superbunch structure. In other areas, the evolution of precision requirements (M_W) and the emergence of whole new fields of study (B physics) motivate a redesign. The replacement of the non-magnetic inner tracking detector with a high precision integrated tracker with solenoidal field will enhance identification and measurement of electrons and muons, allow the in situ calibration of the calorimetric energy scale to the level necessary for a substantial reduction in the M_W error, and make the whole area of B physics studies accessible. In the following the different upgrade projects will be discussed.

Muon System

One of the strong features of the DØ detector is its complete muon coverage. Three superlayers of proportional drift tubes, one inside and two outside of a 1.5 m shell of toroidally magnetized steel, provide momentum determination for muons penetrating the 7-10 interaction length thick calorimeter.

The muon system upgrade consists of a change to a faster gas, reducing the maximum drift time from 1.2 μ s to 700 ns, and complete coverage of the detector periphery with a layer of plastic scintillator read out with wave length shifting fibers and phototubes. The scintillator improves the rejection of cosmic rays and will allow unambiguous association of a given track with a particular bunch crossing.

In the forward region, a pad chamber system will increase the trigger rate capability of the detector, to accommodate the high rates associated with B-production.

The detector readout system will also have to be modified, to allow baseline interception during the 2.1 μ s superbunch gap (the current system needs 2.5 μ s) and to implement front-end buffering of bunch crossings during the trigger level 1 decision time.

Calorimeter Electronics

The DØ uranium liquid argon sampling calorimeter is hermetic, has excellent resolution and linearity, and is intrinsically radiation hard; therefore no upgrades or modifications are needed for the detector hardware itself. The front-end electronics, though, has to be completely replaced, due to the shortened bunch crossing interval. The shaping time will be reduced to 400 ns, and, similar to the muon system, analog buffering is needed to allow for the level 1 decision time while further bunch crossings from the same superbunch occur.

Extensive simulation studies have shown that no significant deterioration of the energy resolution will occur due to the shortened charge integration time or the presence of multiple interactions. This is important especially for the precise M_W determination in $W \rightarrow e\nu$ decays.

Trigger and Data Acquisition

Key features of the current DØ trigger and DAQ system are its multilevel architecture

with parallel readout paths for the different detector elements. Its modularity and inherent flexibility permit the retention of the basic system architecture and most of the hardware components for the upgrade. Currently, a maximum trigger rate out of level 1 of 160 Hz can be tolerated, resulting in a rate to tape (after level 2 reduction) of about 2 Hz. At a luminosity of $10^{32} \text{cm}^{-2} \text{s}^{-1}$, high P_T physics alone (W, Z, top) accounts for roughly 3 kHz of level 1 rate, and B physics triggers will bring the total to around 10 kHz. Besides more front-end analog buffering, digital buffering capacity will be increased for the higher trigger levels, and the level 1.5 trigger, which currently delivers a coarse estimate of muon momenta, will be expanded to deal with and combine calorimetric and inner tracking information, allowing a reduction in rate of muon, electron and jet triggers, and combinations thereof, into the level 2 system. Low momentum track triggers for level 1 and level 1.5 will be implemented by processing the fast signals from the scintillating fiber tracker VLPC readout through field programmable gate arrays. The current level 2 trigger system consists of an array of 50 VAX-architecture based processors, which have the full detector information available for background rejection based on fast reconstruction. For the upgrade, more buffering (memory) will be added, key components determining the readout speed will be upgraded, and the processors will be replaced by a RISC-based design (DEC-AXPs).

The Integrated Tracker

The central tracking detectors of the $D\bar{O}$ experiment, located in the small volume of 156 cm diameter of the inner bore of the central calorimeter cryostat, will be replaced by an integrated magnetic tracking system. Figure 2 shows a quarter of the longitudinal detector cross section. Particles emerging from the interaction region encounter:

- A silicon microstrip tracker, with $50 \mu\text{m}$ pitch, consisting of four concentric 84 cm long barrels¹, at radii of 3, 5, 7, and 9 cm, with interspersed disks. Four more disks at each end bring the total length of the central silicon detector to 120 cm, and in the far forward region larger disks at a distance of 125 cm from the nominal interaction point give additional coverage for the pseudorapidity region from 2 to 4. The central disks and half of the barrel layers are double sided, providing small angle stereo measurements. The detectors have AC coupled readout to radiation hard SVX-II chips currently under development at FNAL and LBL.
- The scintillating fiber tracker, consisting of four superlayers of $835 \mu\text{m}$ diameter plastic fibers. Barrel lengths range from 220 cm to 254 cm. Each superlayer consists of 8 fiber layers: two axial doublets, separated radially by 1.6 cm to allow reconstruction of a local $R\Phi$ track vector, and two 2° stereo doublets. The layers in each doublet have a half-fiber offset, leading to an effective width of $435 \mu\text{m}$ of the half-cell as basic tracking element. High photon yield multicladd fibers, combined with the readout via VLPCs (Visible Light Photon Counters), fast cryogenic solid state detectors with quantum efficiency better than 60%, result in an average of more than 10 photoelectrons per minimum ionizing particle traversing a fiber, thus leading to a compact fast tracker with high efficiency, good resolution, and excellent trigger and pattern recognition capabilities.

¹An important accelerator parameter strongly influencing the layout of the inner tracking detectors is the axial extent of the interaction region; its rms value of 22 cm directly drives the length of the silicon tracker.

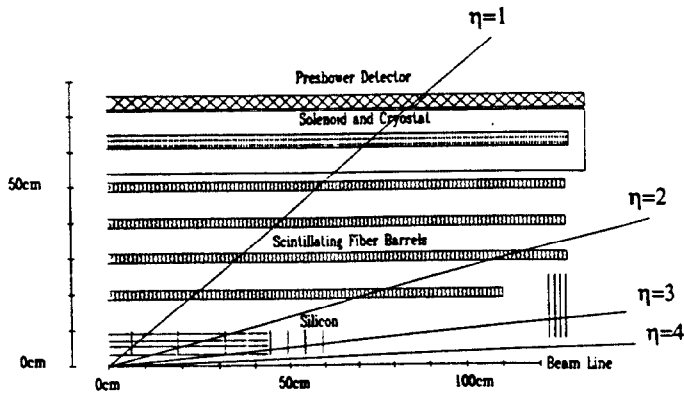


Figure 2: Quadrant view of the integrated tracker

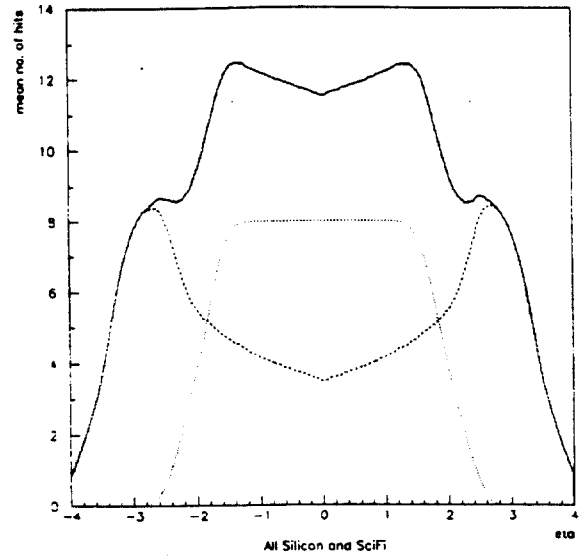


Figure 3: Number of axial track measurements for the central tracker, as function of pseudorapidity

- The 2.5 m long superconducting solenoid delivering a homogenous field of 2 Tesla. Augmented by a tapered layer of lead placed outside the cryostat for the coil, it forms the $2 X_0$ radiator/converter for
- The preshower detector. Electron identification and background rejection (π^\pm/π^0 overlap, and early π^\pm charge exchange in the calorimeter), recovery of electromagnetic energy otherwise lost due to the coil and the cryostat walls, and improvement of photon- π^0 separation (on a statistical basis) are the main reasons for incorporating a preshower detector in the design of the magnetic tracker. Located immediately in front of the central calorimeter cryostat, it is constructed of one axial double layer and two 20° stereo double layers of 5 mm wide scintillator strips, read out with scintillating fibers into VLPCs. The intrinsic resolution of 0.5 mm in $R\Phi$ and 1.1 mm in the axial coordinate is well matched to the tracking resolution. A test beam experiment showing excellent pion-electron pulse height separation capability has been conducted, at that time using multi anode photo tubes instead of high QE VLPCs.

Front-End Readout Electronics for the Tracking Detectors

All three tracking detectors (silicon, fiber tracker, preshower) will use similar front-end electronics. The preshower detector and the fiber tracker share the cryogenic VLPC system, and both the silicon and the fiber-VLPC-based detectors will probably use the high density SVX-II chip, which incorporates 128 channels of preamplifier, switched capacitor array storage and 8 bit ADC, together with a readout multiplexer, into a single radiation hard integrated circuit. For the first-level fiber-tracker trigger, a fast digital pickoff is needed; design options

for the trigger circuitry are currently under investigation. For all three detectors, optical fibers will provide the path to the VME based DØ data acquisition system. From the VME receiver cards, the data are available for the Level 1.5 and Level 2 trigger processors and logging to tape.

Simulation Studies

The simulation studies use a detailed GEANT-based description of the detector, including a representation of passive materials, magnetic field inhomogeneities, low energy particles, and realistic detector effects, including conservative estimates of the amount of dead channels and extra noise hits. The event simulation is followed by prototype versions of the pattern recognition and track fitting packages. The optimization of the detailed physical layout of the tracker has been studied using a parametrized version of the tracking.

Acceptance, Occupancies, Single Particle Resolution

The scintillating fiber detector and the central part of the silicon detector fully cover the rapidity region $|\eta| < 2$. As figure 3 shows, beyond $|\eta| = 2$ the forward silicon disks are essential to achieve a sufficient number of measurements on a track, due to the large axial extent of the interaction zone. Occupancies are low: for $t\bar{t}$ events, silicon occupancies range from 0.2 to 0.5%, depending on barrel layer, and for the SciFi layers from 2 to 6%. The track reconstruction efficiency for particles traversing all four SciFi barrels has been shown to be around 98%. This result proved to be very robust against variations in signal reducing effects in the light transport and VLPC readout system. The P_T resolution for tracks with $|\eta| < 1.5$ is $(\frac{\sigma(P_T)}{P_T})^2 = (0.01)^2 + (0.0022 \cdot P_T)^2$; for comparison, the resolution of the present external muon tracker is $(\frac{\sigma(1/p)}{1/p})^2 = (0.18)^2 + (0.01 \cdot p)^2$.

Mass Resolution

Mass resolution has been studied for a whole range of massive objects, from 3 to 350 GeV/c², in their decay to $\mu^+\mu^-$. Figure 4 shows the J/Ψ mass resolution for two classes of events: central events, where both muons have traversed all four SciFi barrels, and the complementary class. Also shown are the pseudorapidity distributions of the muons for both cases.

B Tagging

B-quark tagging via impact parameter measurement relies on the high intrinsic resolution of the silicon detector (8 μm); it will be an important tool in identifying top decays. A model algorithm requiring three or more tracks in a b-jet reconstructed with $P_T > 1$ GeV and impact parameter significance greater than three was studied. For $t\bar{t}$ events with $M_{\text{Top}} = 150$ GeV/c², the tagging efficiency is 79%, with the loss mainly due to the $P_T > 1$ GeV requirement. The probability to mistag a background event from associated production of W+jets is about 1%.

Top Discovery and Mass Determination

Defining as criterion for top discovery the observation of at least five dilepton events, plus 40 lepton+jets events, the range accessible for DØ evolves as follows with integrated luminosity: for 100 pb⁻¹ it extends to 165 GeV/c²; for 250 pb⁻¹ to 195 GeV/c²; and with 1 fb⁻¹ the whole range allowed by the standard model (with one Higgs doublet) is covered, up to top masses of 235 GeV/c². The top mass determination will be improved by the ability to tag b-jets. B-tagging in W+jets events reduces the combinatorial background in W-jet pairing, improving the mass resolution for the signal content from $t\bar{t} \rightarrow WbWb \rightarrow e\nu b + \text{jets}$. An error of 5 GeV is believed to be obtainable from the electron+jets data sample alone.

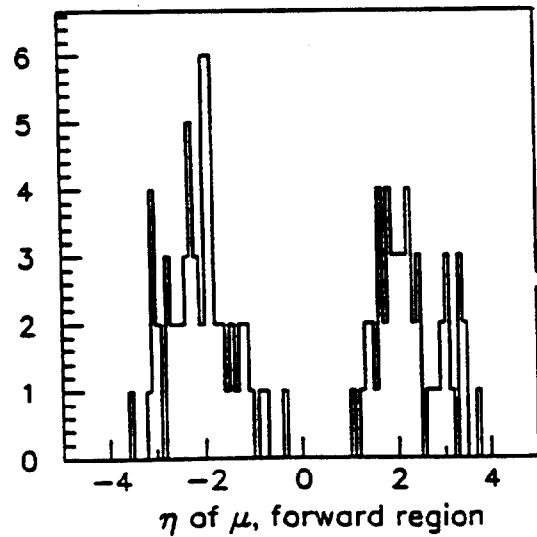
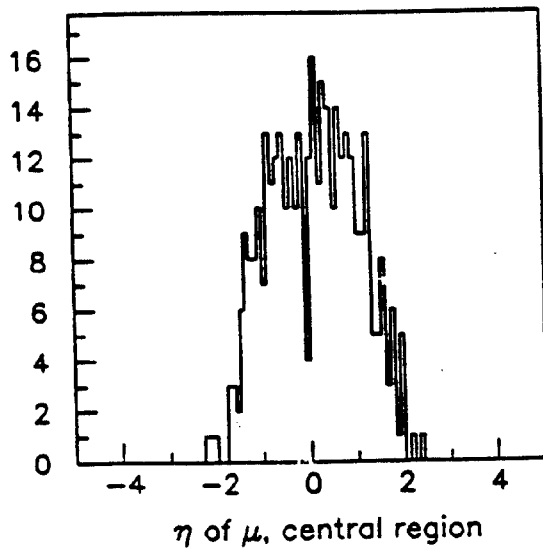
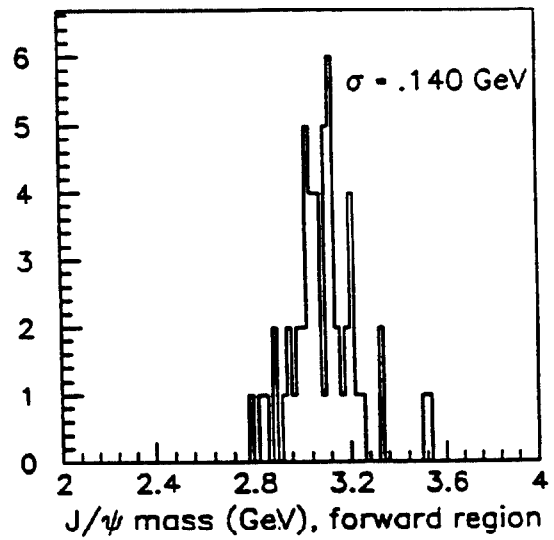
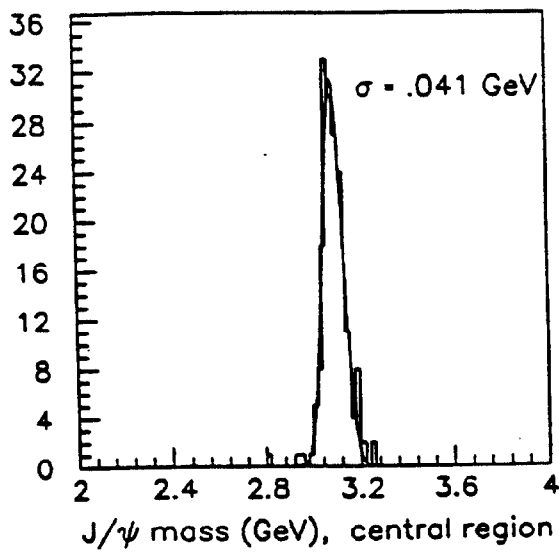


Figure 4: J/ψ mass resolution and corresponding η distribution of muons; left: central, right: forward J/ψ sample; cf. text

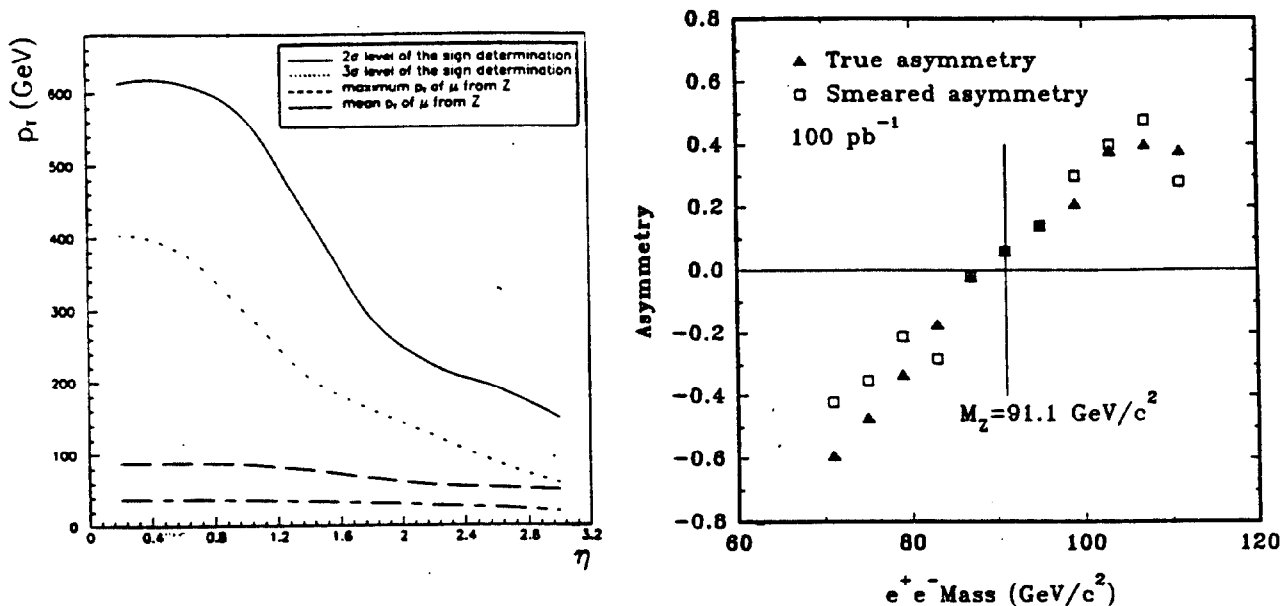


Figure 5: left: lepton P_T from Z^0 decay, and fiducial P_T range for charge sign determination, as function of pseudorapidity; right: forward-backward asymmetry vs. pair mass

e^+e^- Forward-Backward Asymmetry

Another measurement of high interest among tests of the standard model is the determination of the forward-backward asymmetry in $\bar{p}p \rightarrow Z/\gamma^* \rightarrow e^+e^-$. The asymmetry at the Z^0 pole is directly related to $\sin^2 \theta_W^{\text{eff}}$. The charge sign determination for the Z^0 decay products is possible over the full rapidity range covered by the $D\phi$ electromagnetic calorimeter, as figure 5a illustrates. Figure 5b shows the asymmetry as function of the mass of the e^+e^- pair, both for the generated and for the reconstructed event samples. An integrated luminosity of 1 fb^{-1} will allow a determination of $\sin^2 \theta_W^{\text{eff}}$ with an error of 0.001.

As mentioned earlier, this and other measurements can be used for a consistency check on the electroweak standard model; in particular the measurements of M_W , M_{Top} and $\sin^2 \theta_W^{\text{eff}}$ can be combined to perform this check in a single experiment.

B Physics

At a luminosity of $10^{32} \text{ cm}^{-2} \text{ s}^{-1}$, 10^{11} b hadrons per year are produced at the Tevatron; this high yield permits a very broad range of studies, some of them inaccessible to e^+e^- colliders running on the $\Upsilon(4S)$. Examples are:

- B_s mixing, determination of V_{ts}
- B_c studies
- b-baryon spectroscopy
- Rare decays involving flavour changing neutral currents

Figure 6 displays the results of a MonteCarlo study of $B_s\bar{B}_s$ oscillations. One B_s is reconstructed from the decay $B_s \rightarrow D_s\pi\pi\pi, D_s \rightarrow \Phi\pi$, the other $B_s(\bar{B}_s)$ provides the particle-antiparticle lepton tag. It is estimated that 1 fb^{-1} will deliver ≈ 5400 B_s pairs with a lepton

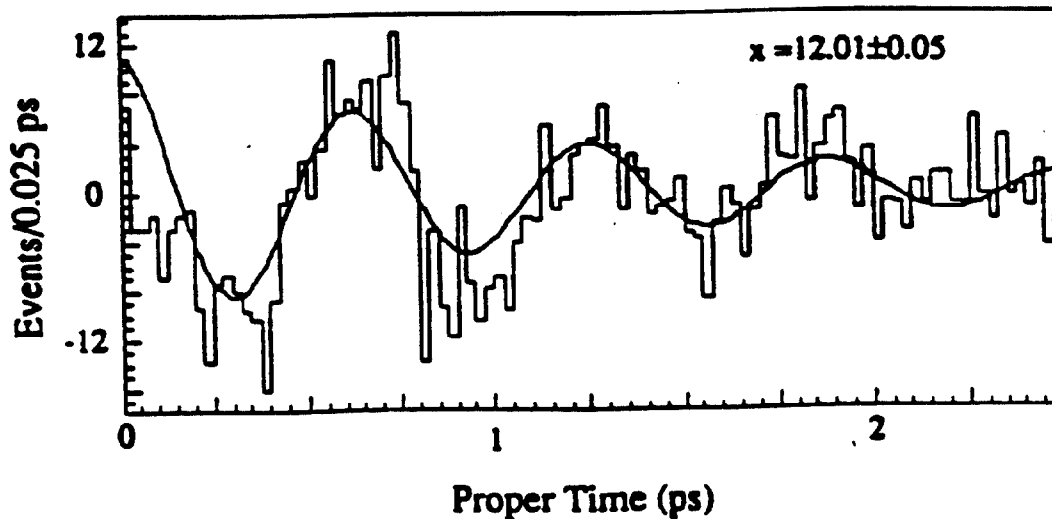


Figure 6: B_s mixing in the upgraded $DØ$ detector; see text

tag.

CP violation

Study of CP violation in the B system probably puts the most stringent requirements on the trigger and data acquisition rate capability of a hadron collider detector. Simulation studies have been done using the decay $B \rightarrow J/\Psi K_S$. Figure 7 shows the mass distributions for the J/Ψ , the K_S , and the B-meson, the latter with and without mass constraints on the Kaon and J/Ψ . The mass resolutions obtained from the simulation are 50 MeV for the J/Ψ , 6 MeV for the K_0 , 70 MeV for the B without Kaon and J/Ψ mass constraint, and 20 MeV with such constraints. With $1 fb^{-1}$ of data, $DØ$ should be able to determine $\sin 2\beta$ with an uncertainty of about 0.15.

Conclusion

An ambitious upgrade and physics program has been proposed for the $DØ$ experiment, and, as of November 1993, been approved.

The upgrade combines a new high precision magnetic tracker based on silicon and scintillating fiber detectors in a 2 T solenoidal field and a preshower detector with existing hermetic liquid argon calorimetry and muon systems. The detector will provide a powerful facility for the study of high P_T phenomena and B physics in the era of the Tevatron main injector. The $DØ$ upgrade is described in detail in references [2-7], from which the results presented here have been extracted.

References

1. The $DØ$ Detector, S. Abachi et al., to be published in NIM (1993).
2. The $DØ$ Upgrade, unpublished (1990).
3. P823 ($DØ$ Upgrade): Responses to the Physics Advisory Committee, $DØ$ note 1148 (1991).
4. E823 ($DØ$ Upgrade): R&D and Optimization Progress Report, $DØ$ note 1322 (1992).
5. E823 ($DØ$ Upgrade): Step-1 and Beyond, $DØ$ note 1421 (1992).
6. E823 ($DØ$ Upgrade): $DØ_\beta$, $DØ$ note 1733 (1993).
7. Design Report of the 2T Superconducting Solenoid for the $DØ$ Upgrade, J. Brzezniak et al. (1993)

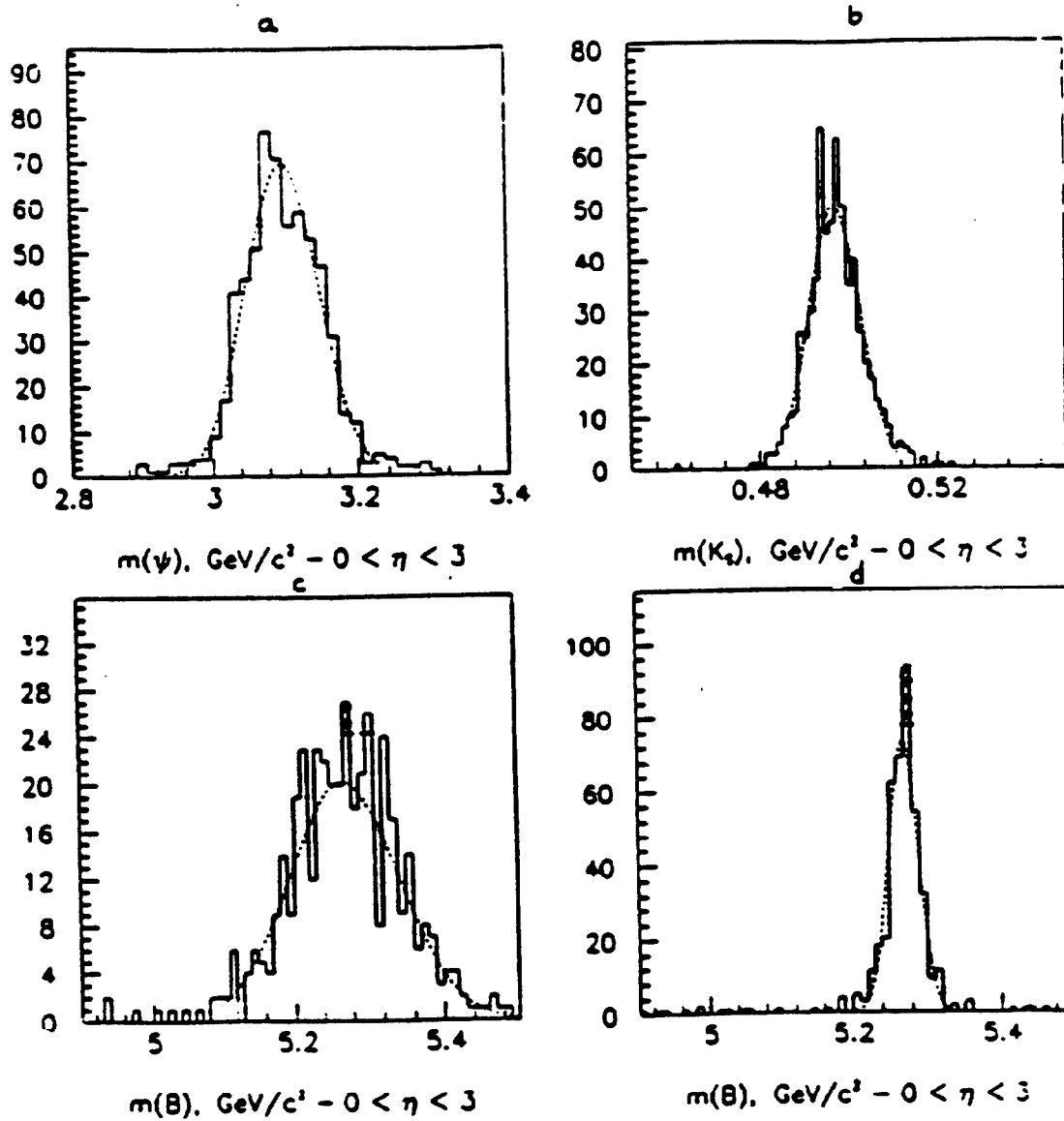


Figure 7: mass spectra for reconstructed events $B \rightarrow J/\Psi K_0$